Model-potential calculations of tunnelling rate constants for the field-ion microscope

1993 J. Phys.: Condens. Matter 5 1195

(http://iopscience.iop.org/0953-8984/5/9/004)

J. Phys.: Condens. Matter 5 (1993) 1195–1202. Printed in the UK

Model-potential calculations of tunnelling rate constants for the field-ion microscope

S C Lam and R J Needs
Cavendish Laboratory, University of Cambridge, Cambridge CB3 0HE, UK

Received 30 September 1992, in final form 7 January 1993

Abstract. We have performed tunnelling calculations for the field-ion microscope using the JWKB method of Haydock and Kingham and the model potentials introduced by Homeier and Kingham. We have found that Homeier and Kingham overestimated the cross-surface variations in the tunnelling rate constant by a factor of up to five. The reasons for these inaccuracies are analysed and we give the results of more accurate calculations.

The main goal of theoretical studies of imaging in the field-ion microscope (FIM) has been to explain the observed image contrast from calculations of the cross-surface variations in the rate of ionization of imaging gas atoms [1]. Two factors contribute to the image contrast: (1) the probability that an imaging gas atom is present at a particular location, and (2) the probability that the imaging gas atom will be field ionized. One of the important developments has been improved calculations of tunnelling rate constants for gas atom ionization in the FIM. Haydock and Kingham [2] developed a simple JWKB approximation which is suitable for calculating tunnelling rate constants in the FIM and applied it to a model potential for a flat surface. This work was further developed by Kingham and collaborators in a series of papers, perhaps the most important of which was by Homeier and Kingham [3], who calculated the tunnelling rate constants for various corrugated model potentials which simulated the atomic structure of real surfaces. This work was important because it produced large cross-surface variations in the tunnelling rate constant which, according to Homeier and Kingham, 'may be sufficient to explain the observed contrast of the field-ion microscope' [3]. Indeed this work was used as a significant part of the theoretical picture developed and reviewed by Forbes [1], in which he concluded that local contrast under normal operating conditions is determined by the rate constant mechanism. However, this conclusion has not been universally accepted, and Tsong [4] has claimed that the image contrast may arise from an enhancement in field ionization by field adsorption of imaging gas atoms.

In this paper we show that in their model calculations Homeier and Kingham overestimated the cross-surface variations in the tunnelling rate constant by a factor of up to five in some cases. We calculate more accurate tunnelling rate constants and briefly discuss the implications of our results for theoretical understanding of the imaging process in the FIM. We have studied the model potentials of corrugated surfaces introduced by Homeier and Kingham and have used the same JWKB formalism for the tunnelling calculations, but our work differs from theirs in the

0953-8984/93/091195+08$07.50

accuracy of evaluation of the rate constant expressions. Although the numerical differences between our results and those of Homeier and Kingham are large we still believe that it is possible that local contrast under normal operating conditions is essentially determined by the rate constant mechanism.

First we give a brief description of the JWKB formalism of Haydock and Kingham [2]. In this scheme the tunnelling rate constant, R, is given by a summation of one-dimensional contributions from infinitesimal solid angles:

$$R = A^2\nu \int_{\phi=0}^{\phi=2\pi} \int_{\theta=0}^{\theta=\pi/2} \exp\left[-2^{3/2} \int_{r_0(\theta,\phi)}^{r_1(\theta,\phi)} [V(r,\theta,\phi) - E]^{1/2} \mathrm{d}r \right] \sin\theta \, \mathrm{d}\theta \, \mathrm{d}\phi \tag{1}$$

where $r_0(\theta, \phi)$ and $r_1(\theta, \phi)$ are respectively the inner and outer classical turning points along the direction (θ, ϕ), and $V(r, \theta, \phi)$ is the total potential felt by the tunnelling particle whose energy is E. The prefactor $A^2\nu$ has been taken to be a constant for all the results presented in this paper. We have discussed appropriate values for this prefactor in a previous paper [5], finding it to be strongly dependent on the ionization energy of the imaging gas atom, but only weakly dependent on the magnitude of the applied field. This tunnelling scheme has been shown to give excellent results for the uniform-field ionization of hydrogenic atoms [2,5].

Haydock and Kingham applied their JWKB scheme to the case of tunnelling in an FIM using a simple model potential, V_a, for a flat metal surface under a perpendicular applied electric field, given by

$$V_a(x, y, z) = \begin{cases} Fz & z \geqslant 0 \text{ outside metal} \\ -\Phi & z < 0 \text{ inside metal} \end{cases} \tag{2}$$

where F is the magnitude of the electric field and Φ is the workfunction of the metal. To form the full tunnelling potential they added to V_a the potential due to the imaging gas atom which was represented by a hydrogenic potential with effective charge Z_{eff}. For this tunnelling potential they obtained an analytic approximation for the tunnelling rate constant given by equation (1) (equation (9) of [2]).

To calculate the tunnelling rate constants for corrugated surfaces Homeier and Kingham used the expression derived for the flat surface, into which they inserted values of the electric field at the gas atom nucleus and the width of the tunnelling barrier normal to the surface appropriate for the corrugated surface. This procedure may be reasonable if the tunnelling is extremely well directed along the direction of the surface normal, but in fact the tunnelling is significant over angles of up to about 30° to the surface normal. The effect of this approximation is to overestimate the rate constant when the gas atom is above a protrusion, which leads to an overestimate of the cross-surface variations in the rate constant.

There is a second significant source of error in Homeier and Kingham's calculations. As is discussed in detail in [5], the analytic expression derived by Haydock and Kingham for the tunnelling rate constant above a flat surface mentioned above is highly inaccurate. The main problem with their expression is that the tunnelling rate constant rises too steeply as the imaging gas atom approaches the metal surface. This leads to results which are far too sensitive to variations in the thickness of the tunnelling barrier and therefore to a significant overestimation of the cross-surface variations in the tunnelling rate constant. We have developed a much

better analytic approximation (equation (5) of [5]) which does not suffer from this flaw which, for completeness, we reproduce below:

$$R(z_0) \simeq [3\pi A^2 \nu F(16B^2/Z_{\text{eff}}F)^{Z_{\text{eff}}(2/B)^{1/2}}/2^{3/2}] \exp[Z_{\text{eff}}(2/B)^{1/2}]$$
$$\times ([\exp(-2^{5/2}B^{3/2}/3F) - \exp(-2^{5/2}B^{3/2}/3F\cos\theta_s)]/B^{3/2}$$
$$+ [\![\exp\{-2^{5/2}[B^{3/2} - (B - Z_{\text{eff}}F\cos\theta_s/B - Fz_0)^{3/2}]3F\cos\theta_s\}]\!]$$
$$\times [B^{3/2} - (B - Z_{\text{eff}}F\cos\theta_s/B - Fz_0)^{3/2}]^{-1}) \tag{3}$$

$$\theta_s = \begin{cases} 0 & \text{if } (Bz_0 - Fz_0^2)/Z_{\text{eff}} \geqslant 1 \\ \pi/2 & \text{if } (Bz_0 - Fz_0^2)/Z_{\text{eff}} \leqslant 0 \\ \cos^{-1}[(Bz_0 - Fz_0^2)/Z_{\text{eff}}] & \text{otherwise} \end{cases}$$

where z_0 is the distance of the gas atom from the surface and B is its first ionization energy.

We have pointed out two separate effects in Homeier and Kingham's calculations which both tend to overestimate the cross-surface variations in the tunnelling rate-constant. We now proceed to give results of more accurate calculations for the same model potentials as they used. Homeier and Kingham investigated five separate models, a flat surface (model a), three models of a surface protrusion with axial symmetry (models b, c and d) and a model of an atomic step (model e), although in the latter case they did not give results for tunnelling rate constants. Potentials for models a–d are illustrated in figure 1 and for clarity we give the expressions for the potentials below. We have not considered the model of the atomic step. The potential for model a is given by equation (1). The metal surface for model b is a hemispherical protrusion on an otherwise flat surface. In spherical polar coordinations (r, θ, ϕ) the potential is

$$V_b(r, \theta, \phi) = -F(r - R_0^3/r^2)\cos\theta \tag{4}$$

where we take the radius of the hemisphere to be $R_0 = 0.158$ nm. Model c is a half spheroid on a plane, and in prolate spheroidal coordinates (η, ξ, ϕ) [6] the potential is given by

$$V_c(\eta, \xi, \phi) = \tfrac{1}{2}F\eta[\![\xi_0\{\xi \ln[(\xi + 1)/(\xi - 1)] - 2\}$$
$$\times \{\xi_0 \ln[(\xi_0 + 1)/(\xi_0 - 1)] - 2\}^{-1} - \xi\}]\!] \tag{5}$$

where we choose $\xi_0 = \sqrt{2}$. The prolate spheroidal coordinates (η, ξ, ϕ) are related to a Cartesian system by

$$x = \tfrac{1}{2}a[(\xi^2 - 1)(1 - \eta^2)]^{1/2}\cos\theta$$
$$y = \tfrac{1}{2}a[(\xi^2 - 1)(1 - \eta^2)]^{1/2}\sin\theta \tag{6}$$
$$z = \tfrac{1}{2}a\xi\eta$$

where $a = 2R_0$, and again we choose $R_0 = 0.158$ nm. In cylindrical polar coordinates (ρ, θ, z) the potential for model d is given by

$$V_d(\rho, \theta, z) = -F[z - a\exp(-kz)J_0(k\rho)] - V_0 \tag{7}$$

where J_0 is a Bessel function and we use $k = 12.6$ nm^{-1}, $a = 72.8$ pm and $V_0 = -1.19$ eV. In each case the metal surface is taken as the zero of potential and far away from the surface the electric field has magnitude F and is directed along the surface normal. Inside the metal the potential is taken to be equal to the negative of the workfunction.

We use an atomic ionization energy of 24.5 eV and an electric field of 45 V nm^{-1}, which are appropriate for imaging with He atoms, and a metal workfunction of 4.5 eV. First we consider the case when the imaging gas atom is on the critical surface, which is the surface on which the atomic ionization energy is equal to the Fermi level of the metal. The rate constants were calculated for an He atom at the characteristic points on the critical surface shown in figure 1. For model d the points P_2, P_3, P_4 and P_5 are respectively 0.3 nm, 0.56 nm, 0.81 nm and 1.06 nm away from P_1. In table 1 we give results for the tunnelling rate constants calculated using three methods. The results labelled (HK) were obtained using precisely the same procedure and tunnelling rate constant expression adopted by Homeier and Kingham, while those labelled (LN) were obtained in the same manner but using the more accurate analytic expression of Lam and Needs [5]. The results labelled (N) were obtained by a full numerical evaluation of equation (1).

The large differences between the data labelled (HK) and (N) in table 1 indicate that Homeier and Kingham overestimated the cross-surface variations in the tunnelling rate constant by a factor of up to five in some cases. The results obtained using our more accurate analytic approximation (LN) are in much better agreement with the numerical results (N), although there is still a tendency to overestimate the variations in the rate constant. These results indicate that the most important defect of Homeier and Kingham's calculations was the use of the poor analytic approximation for the rate constant expression for the flat surface.

It is difficult to estimate the magnitude of the cross-surface variations in the rate constant required for atomic resolution in the FIM, although Forbes [1] suggested that the minimum required variation would be roughly a factor of two. The actual contrast achieved in experiments is also uncertain, although Tsong quotes an experimental contrast of at least a factor of ten [7]. If we accept the latter value we should conclude that the cross-surface variations in the tunnelling rate constant that we have found might be sufficient to explain the atomic resolution of the FIM. An additional problem is that it is difficult to assess the accuracy of the model tunnelling potentials introduced by Homeier and Kingham. We have also performed tunnelling calculations for the FIM using potentials obtained from self-consistent electronic structure calculations which include the full screening of the applied electric field [8]. Calculations for imaging of an adatom on an Al surface with He atoms and an electric field of 30 V nm^{-1} gave a ratio of the tunnelling rate constant on top of the adatom to the value above the flat surface of roughly seven, which is smaller than the values of 19 for model b and 104 for model c obtained under the same imaging conditions and using numerical evaluation of equation (1). Larger cross-surface variations would be obtained from the self-consistent potentials if the surface atomic species was W or Ir, which might possibly give values as large as those obtained for the corrugated model potentials.

Another quantity of interest is the energy distribution of ionized gas atoms arriving at the detector. Measurements of the width of this distribution give values as small as 0.8 eV for imaging with He atoms and an electric field of 45 V nm^{-1} [9]. This narrow energy distribution implies that the region above the surface in which most of the ionization occurs (the ionization zone) is about $0.8/45 \simeq 0.02$ nm wide. If we further

Table 1. The relative field strength on the critical surface, the distance of the critical surface from the metal surface and the tunnelling rate constant for the four model potentials a–d, for imaging with He atoms, an electric field of 45 V nm^{-1} and a metal workfunction of 4.5 eV. The positions of the characteristic points, P, are shown in figure 1. The rate constants were calculated using Homeier and Kingham's scheme (HK), using the same method but with the more accurate rate constant expression of Lam and Needs (LN), and from a full numerical evaluation of the rate constant expression (N). Values are given relative to those for model a of a flat surface.

		Model							
Characteristic point		(a) P	(b) P	(c) P	(d) P_1	(d) P_2	(d) P_3	(d) P_4	(d) P_5
Relative field strength		1	1.079	1.158	1.0024	0.9990	1.0007	0.9994	1.0006
Critical distance (nm)		0.444	0.306	0.257	0.414	0.477	0.433	0.462	0.436
Relative tunnelling rate constant	$Z_{eff} = 1$ (HK)	1	74.92	477.0	2.230	0.5172	1.366	0.701	1.269
	(LN)	1	37.2	194	1.71	0.683	1.20	0.786	1.15
	(N)	1	24.3	125	1.56	0.797	1.15	0.874	1.11
	$Z_{eff} = 1.5$ (HK)	1	70.79	427.6	2.226	0.5176	1.365	0.701	1.269
	(LN)	1	21.7	102	1.56	0.952	1.22	0.970	1.10
	(N)	1	19.0	83.0	1.48	0.809	1.14	0.884	1.10

assume that the width of the ionization zone is directly related to the width of the region in which the ionization rate constant is large then we would conclude that this region is also very narrow, presumably of the order of 0.02 nm wide. We believe that it is important to give a satisfactory account of the width of the ionization zone, both because it is related to a directly measurable quantity and because it is related to the cross-surface variations in the tunnelling rate constant. The cross-surface variations in the tunnelling rate constant derive essentially from variations in the thickness of the tunnelling barrier over the surface. Presumably the width of the ionization zone is determined by the rate of decrease of the rate constant with increasing thickness of the tunnelling barrier, which is therefore related to the cross-surface variations in the tunnelling rate constant.

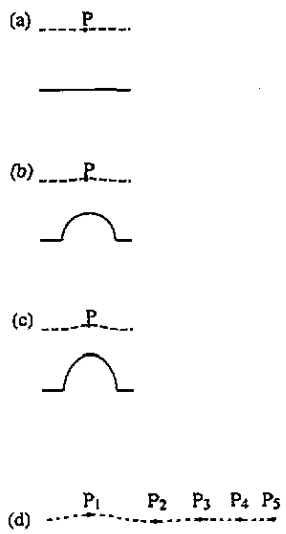

Figure 1. The four model potentials a–d used in the tunnelling calculations. In each case the solid line represents the metal surface, which is taken to be the zero of potential, while the dotted line represents the critical surface. The points labelled P are those at which the tunnelling rate constant is given in table 1.

In figure 2 we plot the tunnelling rate constant versus the distance of an He atom from the critical surface for models b and c where we take the gas atom to be above the centre of the surface protrusion. These calculations are for imaging with He and $F = 45$ V nm^{-1}, $\Phi = 4.5$ eV, and $Z_{\text{eff}} = 1$. The full-width-at-half-maximum (FWHM) of the peak in the tunnelling rate constant is 0.04 nm for model b and 0.033 nm for model c. For the flat surface (model a) the rate-constant on the critical surface is less than twice the value far from the surface so that in this case the FWHM is not defined, while for model d the corresponding FWHM above the central protrusion is 0.175 nm. If we use the simple approximation that the width of the energy distribution of ions is given by the product of the applied field and the FWHM of the tunnelling rate constant then we obtain widths of 1.8 eV and 1.7 eV for models b and c, respectively, which are in reasonable agreement with the experimental value of 0.8 eV, whereas model

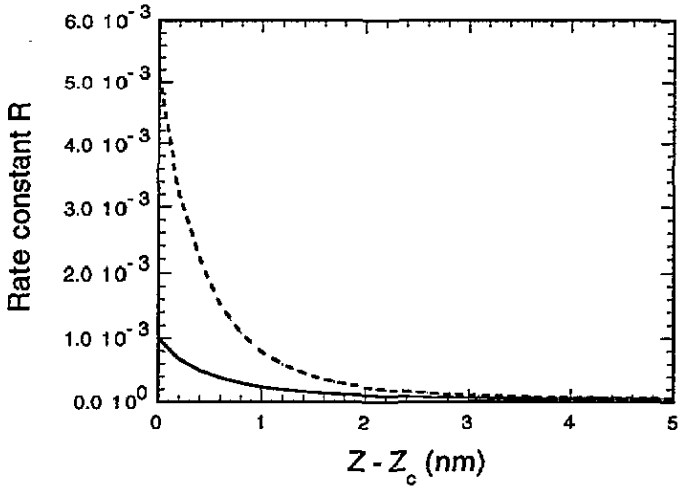

Figure 2. The tunnelling rate constant versus the distance of an He atom from the critical surface for model potentials b (solid curve) and c (dashed curve), with an applied field of $F = 45$ V nm^{-1} and a metal workfunction of $\Phi = 4.5$ eV, and an effective charge on the gas atom of $Z_{\text{eff}} = 1$.

d gives a very large width of 7.9 eV. These results indicate that the ionization zone width is a strongly decreasing function of the corrugation of the surface. This is an important result because previous JWKB tunnelling calculations for flat surfaces have given ionization zone widths which are too large [10]. (We note that the estimates of the width of the ionization zone obtained by Haydock and Kingham for model a [2] are flawed for two reasons: first because they used the inaccurate expression for the tunnelling rate constant, and second because their method of extracting the width leads to large errors. We will discuss the latter point in more detail elsewhere [11].)

In conclusion we have repeated the tunnelling calculations of Homeier and Kingham using more accurate analysis and obtained significantly smaller cross-surface variations in the rate constants. However, we still find cross-surface variations which might be large enough to explain the atomic resolution of the FIM. We have also found that the width of the ionization zone is dependent upon the surface corrugation, and for large corrugations we find widths in reasonable correspondence with experimental values.

This work was supported by the Science and Engineering Research Council (UK). S C Lam thanks the Croucher Foundation for financial support.

References

[1] Forbes R G 1985 *J. Phys. D: Appl. Phys.* **18** 973
[2] Haydock R and Kingham D R 1981 *Surf. Sci.* **103** 239
[3] Homeier H H H and Kingham D R 1983 *J. Phys. D: Appl. Phys.* **16** L115
[4] Tsong T T 1990 *Atom-Probe Field Ion Microscopy* (Cambridge: Cambridge University Press) pp 87–93
[5] Lam S C and Needs R J 1992 *Surf. Sci.* **277** 359
[6] Morse P M and Feshbach H 1953 *Methods of Theoretical Physics* part 2 (Tokyo: McGraw-Hill) p 1284
[7] p 93 of [4]

[8] Lam S C and Needs R J to be published
[9] Müller E W and Tsong T T 1969 *Field Ion Microscopy: Principles and Applications* (Amsterdam: Elsevier)
[10] Lam S C and Needs R J 1992 *Surf. Sci.* **271** 376
[11] Lam S C and Needs R J to be published